Steel and Composite Structures, *Vol. 19, No. 3 (2015) 615-633*
DOI: http://dx.doi.org/10.12989/scs.2015.19.3.615

Behaviour and design of composite beams subjected to flexure and axial load

Brendan Kirkland * and Brian Uy [a]

Centre for Infrastructure Engineering and Safety, *School of Civil and Environmental Engineering*, *Faculty of Engineering*, *The University of New South Wales* (*UNSW*) *Sydney*, *NSW 2052*, *Australia*

(*Received October 16, 2014, Revised February 04, 2015, Accepted February 06, 2015*)

Abstract. Composite steel-concrete beams are used frequently in situations where axial forces are introduced. Some examples include the use in cable-stayed bridges or inclined members in stadia and bridge approach spans. In these situations, the beam may be subjected to any combination of flexure and axial load. However, modern steel and composite construction codes currently do not address the effects of these combined actions. This study presents an analysis of composite beams subjected to combined loadings. An analytical model is developed based on a cross-sectional analysis method using a strategy of successive iterations. Results derived from the model show an excellent agreement with existing experimental results. A parametric study is conducted to investigate the effect of axial load on the flexural strength of composite beams. The parametric study is then extended to a number of section sizes and employs various degrees of shear connection. Design models are proposed for estimating the flexural strength of an axially loaded member with full and partial shear connection.

Keywords: composite beams; combined actions; composite construction; axial force

1. Introduction

Composite steel-concrete beams are being increasingly used in situations in which an axial load may be introduced into the member. Some representative examples include the installation of post-tensioning cables, cable stayed bridges and inclined members in stadia and bridge approach spans. The necessity to transfer diaphragm forces due to wind and seismic loads will introduce an axial load into beams used in floor systems for braced multi-storey buildings. Continuous members may incur axial loads due to thermal expansion or contraction of materials and the restriction of their longitudinal displacement at the supports. In extreme cases where a support is 'removed', beams must withstand high tensile loads to avoid progressive collapse. In all of these situations, the beam may be subjected to any combination of flexure and axial load (Fig. 1). However, modern steel and composite construction codes, including AS2327.1 (Standards Australia 2003) and Eurocode 4 (British Standards Institution 2004), currently do not address the effects of these combined actions.

*Corresponding author, Research Associate, E-mail: b.kirkland@unsw.edu.au
[a] Professor, E-mail: b.uy@unsw.edu.au

Copyright © 2015 Techno-Press, Ltd.
http://www.techno-press.org/?journal=scs&subpage=8 ISSN: 1229-9367 (Print), 1598-6233 (Online)

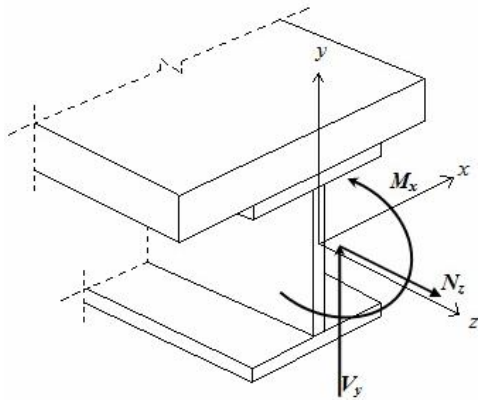

Fig. 1 Member subjected to flexure, shear and axial load

The effect of axial load introduced through the installation of prestressing cables was researched by Troitsky *et al*. (1989), Saadatmanesh *et al*. (1989a, b) and Ayyub *et al*. (1992, b). Similarly, Uy and Craine (2004) and Lorenc and Kubica (2006) compared conventional steel-concrete composite beams with beams post-tensioned using steel prestressing cables. Their studies noted a 15% and 25% increase in sagging flexural strength due to the combined action of axial compression respectively. Chen and Gu (2005) studied prestressed beams subjected to positive moment and observed an increase in the sagging flexural strength of 84% with a further increase of 7% observed by using a draped tendon. Chen (2005) tested prestressed composite beams subjected to hogging moments. It was found that the addition of the external tendons significantly increased the cracking moment resistance of the beams while only slightly lowering its yield moment. Chen *et al*. (2009) later tested two-span and three-span continuous beams with post-tensioning tendons finding an 18% increase in the sagging moment capacity and a 262% increase in the cracking moment at the supports. However, in all of these studies utilising post-tensioning cables, the specimens were subjected to no more than approximately 15% of the axial compressive strength.

Uy and Bradford (1993) employed a cross sectional analysis method for their prestressed composite beam model. This extended upon previous research by including a longitudinal discontinuity at the beam-slab interface to represent the effect of partial shear connection (PSC). Loh *et al*. (2004a, b) also performed experimental and analytical studies on the effect of PSC in hogging moment regions of composite beams. It was found that for beams using lower degrees of shear connection, a significant increase in rotational capacity was achieved with only a slight reduction in peak moment resistance. Later studies also confirmed the results that the ductility of the beam is considerably increased when partial shear connection is used (Uy and Nethercot 2005, Nguyen *et al*. 2009).

Expressions for the interaction of flexure, shear and axial load were developed by Liu *et al*. (2009) and Huang *et al*. (2009) for steel members and reinforced concrete beams respectively. Shanmugam and Lakshmi (2001) completed a thorough review of over 70 papers on steel-concrete composite columns covering both concrete-encased and infilled sections. This showed the extensive research that had been undertaken on axially loaded members. The composite columns in these papers, however, like many recent studies including Elghazouli and Treadway (2008) and Dundar *et al*. (2008) were doubly symmetric as opposed to a typical composite beam, such as the

cross-section used in this study, which is only symmetrical about its *y*-axis.

Uy and Tuem (2006) were the first to address the effect of tension and provide a full moment–axial load interaction diagram for composite beams. A detailed analytical study of composite beams under combined flexure and axial force was performed by two methods: a cross-sectional analysis (CSA) and a rigid plastic analysis (RPA). The CSA calculates the moment–curvature response of the composite beam subjected to any combination of sagging or hogging bending and axial compression or tension. The RPA and CSA in this study show almost identical results for most cases (Fig. 2). The only variation between the CSA and RPA occurred for the sagging bending and axial compression combination where the RPA results were greater than those of the CSA. This was caused by the fact that part of the cross-section was not yielded at the ultimate case, which is contrary to the RPA's fully yielded assumption. Their model was limited to specimens with FSC and also placed the axial load at the level of the plastic neutral axis. Thus it does not include the additional moment induced by an eccentrically placed axial load or its effect on the load carrying capacity.

Wu *et al*. (2002) extended the classical linear theory of composite beams to include the ultimate limit state by the use of a plastic hinge model. Slip along the member was proposed as the sum of slip due to the applied vertical load, the axial load and the slip at the elastic zone/plastic hinge boundary. An equation for the deflection of the beam was also proposed. Wu *et al*. (2004) later showed the model to have perfect agreement with a numerical study for slip in the elastic stage and an excellent agreement for slip at the ultimate stage.

The study contained herein is part of a larger research project aimed to determine the effect of axial load on the ultimate strength of composite beams through a thorough experimental program as well as multiple analytical and numerical models (Vasdravellis *et al*. 2012a, b, c, 2014). These previous studies by the authors investigated the behaviour and design of composite beams under tension and negative bending, tension and positive bending, compression and negative bending and compression and positive bending respectively. Each of the previous studies contains an

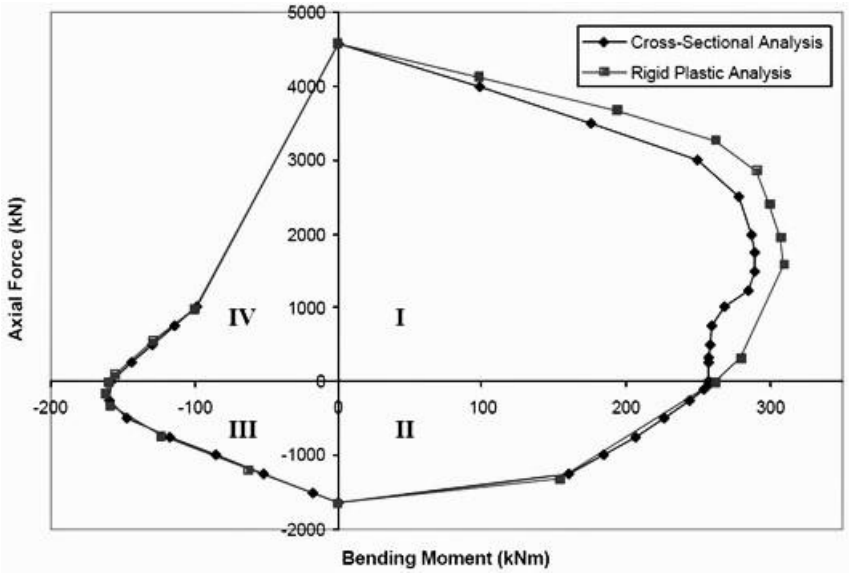

Fig. 2 M–N interaction (Uy and Tuem 2006)

Table 1 Experimental program summary

	Test no.	*N* (kN)	*M* (kNm)		Test no.	*N* (kN)	*M* (kNm)
Series 1 - Negative bending and tension Vasdravellis *et al.* (2012a)	1	0	–161.9	Series 2 - Positive bending and tension Vasdravellis *et al.* (2012b)	1	0	221
	2	–328.5	–174.4		2	–760.5	180.2
	3	–446.5	–151.5		3	–525	223.2
	4	–675.7	–136.2		4	–310	230.2
	5	–1172.7	–101.4		5	–1399.4	47.4
	6	–1497.5	–1.0		6	–1503	7.3
Series 3 - Negative bending and compression Vasdravellis *et al.* (2012c)	1	0	–185.7	Series 4 - Positive bending and Compression Vasdravellis *et al.* (2014)	1	0	222.5
	2	156.1	–148.4		2	229.4	190.4
	3	718.3	–131.1		3	593.8	175.1
	4	1048.3	–78.4		4	1104.8	242.8
	5	1801.1	–38.0		5	1790.9	125.9
	6	2257.7	–11.6		6	2144.1	41.1

experimental series and a finite element analysis of the respective loading combination. The experimental results from those studies are summarised in Table 1.

This paper first presents the developed analytical model and a comparison to the existing experimental results. Results from a parametric study determining the effect of section size and degree of shear connection are given next. Finally, simple design models are proposed for use in practice based on the combined experimental and analytical results which are suitable for inclusion in international design codes.

2. Formulating the analytical model

The developed analytical model simulates the moment–curvature response of a composite beam through a cross-sectional analysis approach using a strategy of successive iterations. This method was previously used by many researchers including Ayyub *et al*. (1992b), Uy and Bradford (1993), Loh *et al*. (2004a, b) and Uy and Tuem (2006). Each solution step requires the principles of equilibrium, compatibility and material stress–strain laws to be satisfied.

The model relies on several important assumptions in its calculations. The first assumption is that no uplift or vertical separation occurs at the steel-concrete interface and the model is thus unable to simulate this behaviour. The model also operates under the assumption that the shear force produced by the applied vertical load is not sufficient to cause shear deformation or reduce the flexural capacity of the section. Because of this assumption, the model is unable to simulate web buckling. Additionally, local buckling at the beam end or premature shear connection failure due to localised strains at the end of the beam are not considered. All of these failure modes were noted during the experimental program.

The developed model extends upon previous research by Uy and Tuem (2006) by including the effects of partial shear connection. It also addresses the moment induced by the eccentrically placed axial load and the effect of this on the load carrying capacity of a member.

2.1 Constitutive relationships

The behaviour of the structural steel and steel reinforcement is generalised by the stress–strain curves obtained throughout the experimental program during the material tests. The constitutive laws employed to represent the stress-strain characteristics of the structural steel and steel reinforcement are presented in Fig. 3(a)-(b). The RPA and CSA as well as the FEA performed by Vasdravellis *et al*. (2012a, b, c, 2014) all utilise material strengths for their respective analysis that were measured during the experimental program for each individual test series. The stress–strain relationship for concrete under compression was recommended by Carreira and Chu (1985)

$$\sigma_c = \frac{f'_c \gamma (\varepsilon_c / \varepsilon'_c)}{\gamma - 1 + (\varepsilon_c / \varepsilon'_c)^\gamma} \tag{1}$$

where

$$\gamma = \left| \frac{f'_c}{32.4} \right|^3 + 1.55 \tag{2}$$

Tension stiffening was modelled using the stress–strain relationship proposed by Kaklauskas and Ghaboussi (2001). The tensile stress is assumed to increase linearly with the same stiffness as the compression case until the concrete cracks at 10% of the ultimate compressive stress. At this point, the stress is reduced by 40% and is then linearly reduced to zero at 10 times the strain where the tensile stress reaches its maximum. Typical stress-strain curves for concrete are shown in Fig. 4.

The model for partial shear connection used by Wu *et al*. (2002) was adapted for this study. This model utilises the classical linear elastic analysis of composite beams and adds a plastic hinge model to augment the analysis at the ultimate limit state. The slip distribution along the length of the member is given by

$$s = s_f + s_n + s_{sp} \tag{3}$$

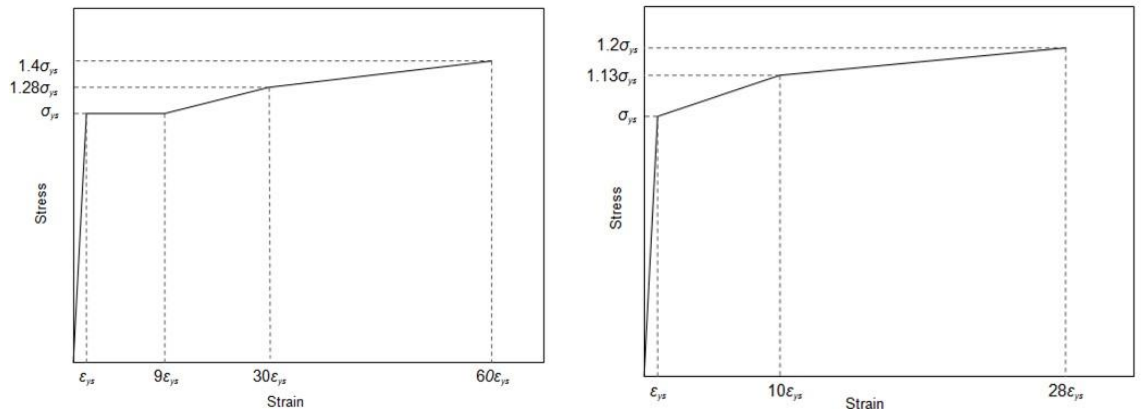

(a) Structural steel (b) Reinforcement

Fig. 3 Material constitutive relationships

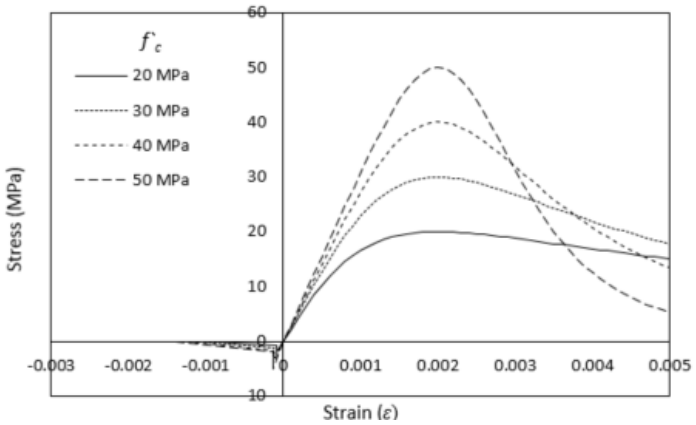

Fig. 4 Stress-strain model for concrete

where s_f, s_n and s_{sp} represent the slip due to the applied vertical load F, axial load N and the slip at the elastic zone/plastic hinge boundary, s_p respectively. The slip distributions are given as

$$s_f = F\frac{\alpha_2}{\alpha_5}\left[1 - \frac{\cosh\left(L\sqrt{\alpha_5}\xi\right)}{\cosh\left(L\sqrt{\alpha_5}\right)}\right] \tag{4}$$

$$s_n = \frac{N\alpha_3}{\sqrt{\alpha_5}}\left[e^{-\left(L\sqrt{\alpha_5}\right)\xi} - 2\cosh\left(L\sqrt{\alpha_5}\xi\right) / \left(e^{2\left(L\sqrt{\alpha_5}\right)} + 1\right)\right] \tag{5}$$

$$s_{sp} = \frac{s_p \cosh\left(L\sqrt{\alpha_5}\xi\right)}{\cosh\left(L\sqrt{\alpha_5}\right)} \tag{6}$$

where L is the length of a shear span, ξ is the dimensionless length parameter, x/L. α_2, α_3 and α_5 are parameters based on the geometric properties of the member given by Wu *et al*. (2002). These equations may be simplified using $\xi = 0$ to obtain the slip at the end of the member. Typical slip distributions along the length of the member are presented by Wu *et al*. (2002). The boundary slip s_p is determined using the relationship between the slip and the axial deformation at a given cross-section. The slip at any cross-section may be determined by the rotation of that cross-section multiplied by the distance between the centroids of the two elements, plus the difference of axial shortening between element 1 and element 2 (Wu *et al*. 2002)

$$s = (d_1 - d_2).\theta + \Delta_1 - \Delta_2 \tag{7}$$

The rotation at the limit of the hinge is equal to the curvature multiplied by the hinge length. The displacement at the limit of the hinge is equal to the strain at the centroid of each element multiplied by the hinge length. Using these two relationships, the slip at the limit of the plastic hinge is given by

$$s_p = (d_w - d_c/2)\kappa L_p + \varepsilon_s L_p - \varepsilon_c L_p \tag{8}$$

where d_w and d_c are the depth of the web and concrete respectively, κ is the curvature and L_p is the length of the plastic hinge. Wu *et al*. (2002) also proposed an equation for the deflection of the beam Δ, where

$$\Delta = \Delta^{P}_{full} + \Delta^{N}_{full} + P g_1(\xi) + N g_2(\xi) + s_P g_3(\xi) \tag{9}$$

where Δ^{P}_{full} is the deflection of the member with full interaction due to the vertical force and Δ^{N}_{full} is the deflection of the member with full interaction due to the eccentricity of the applied axial load. Expressions for the remaining terms g_1, g_2 and g_3 all utilise the geometric properties of the member. These are detailed in Wu *et al*. (2002). The functions g_1 and g_2 approach zero when the stiffness of the shear connectors approaches infinity, which leads to the result given by full-interaction theory (Wu *et al*. 2002). Further information on the partial shear connection model can be found in Wu *et al*. (2001a, b, 2002). The model was shown in Wu *et al*. (2004) to have perfect agreement with numerical studies for slip in the elastic stage and an excellent agreement for slip at the ultimate stage.

2.2 Failure criteria

Failure is considered to have occurred due to one of the following:

- Fracture of the structural steel or reinforcing bar when ultimate strain is reached,
- Slip limit of 10.3 mm. This may occur at the end of the beam or at the boundary of the plastic region, s_p. The value was chosen from the average ultimate slip measured in the push tests.
- Limiting concrete strain is reached. This was chosen as 10,000 $\mu\varepsilon$,
- Limiting deflection is reached. This was chosen as 5% of the beam length,
- Buckling strain has been reached. A prediction of the strain in the compressive flange at the onset of buckling was provided by Kemp (1985). The critical compressive strain, ε_f, was related to the plastic hinge length of a pure steel section under the application of a central point load. The expression was further simplified by Kemp and Nethercot (2001) as

$$\varepsilon_f = 1.33\left(\frac{t_f}{b_f}\right)^2 + 6.6\left(\frac{t_f}{L_p}\right)^2 \tag{10}$$

2.3 Analytical procedures

For the complete evaluation of strain distribution throughout the cross-section, several unknown parameters are required. These were chosen to be the curvature, the bending neutral axis depth, and the slip strain at the interface. The curvature becomes the catalyst for the entire program, and is incremented by 1×10^{-7} only when all equilibrium and compatibility requirements have been satisfied. The model for PSC requires convergence upon the applied vertical load and the length of the plastic hinge. These two values are estimated at the start of each convergence cycle and as such, the bending neutral axis depth becomes the main parameter for convergence to a solution for each curvature increment.

The solution basically requires two iterative loops. The first loop initially increments the curvature. This loop drives the internal second loop by checking the convergence and adjusting parameters to help achieve a successful convergence. Once this has been achieved, it outputs the

desired parameters before incrementing the curvature until failure ceases the analysis.

The second loop receives the curvature, the estimated applied vertical load and the estimated plastic hinge length, then begins to converge upon a unique solution for the bending neutral axis depth.

3. Analytical comparisons with experimental results

The accuracy of the analytical model is validated by comparing it with the experimental results of the 24 composite beam tests, an RPA of the section as well as FEA results presented previously by the authors in Vasdravellis *et al*. (2012a, b, c, 2014).

An RPA of the section was performed with 2 degrees of shear connection; FSC and 0.6 where 0.6 is the degree of shear connection used during the test series for the sagging bending specimens.

The ultimate strength and stiffness determined throughout the test program were all quite accurately predicted by the model. A brief summary of the results obtained by the CSA is shown in Table 2. A complete moment–axial load diagram comparison between the RPA, experiments, FEA and the CSA model is shown in Fig. 5. It can be seen that the degree of shear connection does not affect the ultimate strength in quadrant III. This is attributed to the degree of shear connection, β having been designed for the positive bending case in which the concrete section remains intact. In quadrant III, where all the concrete was cracked at the ultimate case, the shear connection is only required to transfer the tensile strength of the reinforcement. Because of this, the connection is still able to transfer the entire force and is thus considered to exhibit full connection in the hogging moment region. The same is true for large portions of quadrants II and IV, where the concrete was completely cracked at the ultimate case.

The results from the CSA also show an excellent agreement with strain profiles and slip measurements obtained during the experiments (Fig. 6). The failure modes determined by the CSA agreed perfectly with the test results other than those where the limiting deflection stopped the model. The limiting deflection triggered the program to stop in several of the combined load

Table 2 CSA results for test specimens

	Test no.	*N* (kN)	*M* (kNm)		Test no.	*N* (kN)	*M* (kNm)
Series 1 - Negative bending and tension	1	0	-150.4	Series 2 - Positive bending and tension	1	0	246.5
	2	-250	-148		2	-250	235
	3	-500	-139.1		3	-500	215
	4	-750	-119.3		4	-750	190
	5	-1000	-84.8		5	-1000	158
	6	-1250	-48		6	-1250	104
Series 3 - Negative bending and compression	1	0	-150.5	Series 4 - Positive bending and Compression	1	0	243.7
	2	250	-137		2	250	250.1
	3	500	-121.1		3	500	255.4
	4	1000	-103.9		4	1000	234.4
	5	1500	-96.4		5	1500	193.1
	6	2200	-72		6	2200	77

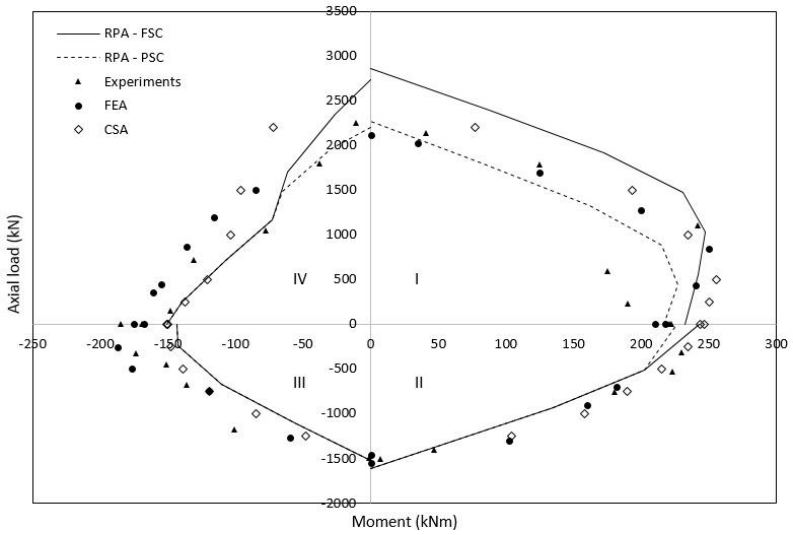

Fig. 5 Comparison of results

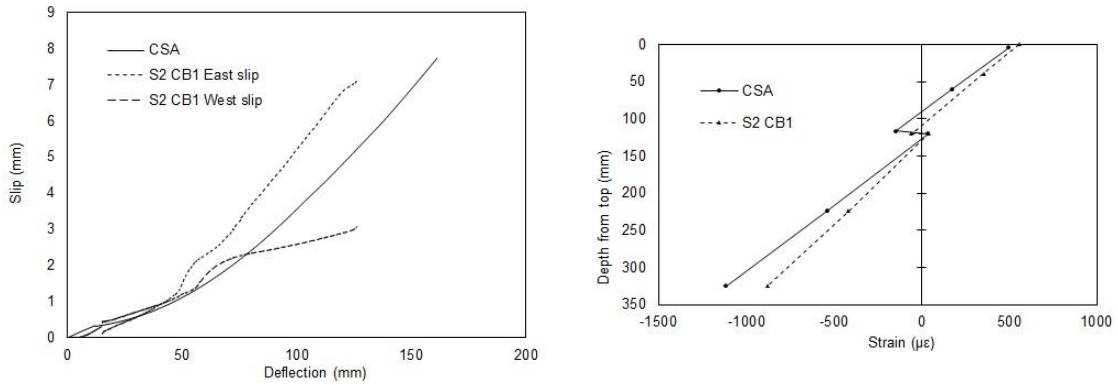

(a) Slip-deflection (b) Strain profile at M = 100 kNm

Fig. 6 Slip and strain comparisons

cases subjected to tension. The limiting strain of the reinforcement and tensile flange were too large to trigger a fracture failure and in some cases may have led to the model slightly overestimating the ultimate strength.

Despite the small variances, the proposed model is considered to be sufficiently accurate and suitable for modelling composite beams with partial shear connection subjected to axial load.

4. Parametric study

Beam compression process was recorded – the axial displacement-shortening and the axial force with the other curve.

Table 3 Parametric study details

No.	Steel section	Span (mm)	Hogging pan (mm)	Sagging span (mm)	b_{cf} (mm)	No. N12 bars	No. studs per shear span			
							FSC	$\beta = 0.8$	$\beta = 0.6$	$\beta = 0.4$
1	200 UB 29.8	8100	2430	5670	600	4	15	12	9	6
2	250 UB 37.3	9300	2790	6510	1000	7	24	20	15	10
3	310 UB 46.2	10600	3180	7420	1500	10	36	29	22	15
4	360 UB 56.7	11900	3570	8330	2000	13	48	38	29	19
5	460 UB 82.1	14400	4320	10080	2000	13	48	38	29	19
6	530 UB 92.4	16200	4860	11340	2000	13	48	38	29	19
7	610 UB 125	18200	5460	12740	2000	13	48	38	29	19

4.1 Rigid plastic analysis

An analytical calculation of the composite beam capacities was conducted by means of an RPA. The sagging moment capacity as a function of the degree of shear connection can be calculated by reducing the concrete force proportionally to β (Standards Australia 2003)

$$F_{cp} = 0.85\beta f'_c b_{cf} D_c \tag{11}$$

The squash load capacity of a section is also determined using Eq. (11). Therefore the axial compressive strength is linearly reduced from N_{uo} for the FSC case to that of the bare steel section N_s at $\beta = 0.0$. The sagging moment capacity is reduced by an average of just 0.9%, 4.4% and 12% for the parametric beams at $\beta = 0.8$, $\beta = 0.6$ and $\beta = 0.4$ respectively as shown in Fig. 7(a). The maximum reductions in the sagging moment capacity all occur in section no. 1 where the respective strengths show a reduction of 1.4%, 6.7% and 16%. The larger sections generally showed less reduction than the small sections. This can be attributed to the concrete component contributing much less strength to the larger sections, and to partial interaction having less influence.

The pure squash load capacity is reduced by an average of 12.5%, 25% and 37.5% for the respective connection strengths. The maximum reductions in squash load capacity all occur in section no. 4, with reductions of 14%, 28% and 42%

A complete moment-axial load interaction diagram is presented in Fig. 8(a)-(b) for $\beta = 1.0$ and $\beta = 0.6$ respectively. In quadrant I of Fig. 8(a), sections 6 and 7 show the greatest increase in sagging moment capacity when axial compression was applied with increases of 20% and 18% respectively. These two sections also show the greatest reduction in the hogging moment capacity when subjected to axial compression seen in quadrant IV. At an axial load of 40% of the squash load, the moment was reduced by 60%. In Fig. 8(b), all values were non-dimensionalised using the results from the FSC case, the pure flexural capacity $M_{uo(\mathrm{FSC})}$ and pure axial capacity $N_{uo(\mathrm{FSC})}$. Similar to Fig. 6, the degree of shear connection does not affect the ultimate strength in quadrant III due to β being designed for the sagging bending case.

4.2 Cross-sectional analysis

CSA results for the reduction in the sagging moment capacity of each section are shown in Fig.

7(b). The figure shows an average of 1%, 6% and 15.9% reduction at β = 0.8, β = 0.6 and β = 0.4 respectively. The maximum reductions for each connection strength all occur in section no. 2, with reductions of 1.3%, 7.8% and 17.9% respectively. The flexural strength determined by an RPA was shown by the CSA to be overestimated in many cases. The CSA showed an average result 1.6% lower than the RPA for β = 0.6 and 4% lower for β = 0.4. The parametric beam with the largest variance was section no. 4 with β = 0.4, which was 9% lower than the RPA result.

A complete moment-axial load interaction diagram is presented in Fig. 8(a)-(b) for β = 1.0 and β = 0.6 respectively. The graph has been non-dimensionalised using the ultimate values for each individual axis that were obtained in the RPA, $M_{uo(\mathrm{RPA})}$ and $N_{uo(\mathrm{RPA})}$. Similar to the RPA results, the larger sections are seen to have the greatest increase in the sagging moment capacity due to axial compression. An increase of 19.5% and 21.7% is seen in Fig. 8(a) at approximately 50% of the squash load for sections 6 and 7 respectively with FSC. The average increase observed in the other sections at 50% of the squash load was just 8.6%, with the lowest being 6.4% in section no. 2. Quadrants II and III show an almost bilinear relationship for all sections. Quadrant IV showed an immediate and dramatic reduction in the hogging moment capacity due to buckling of the

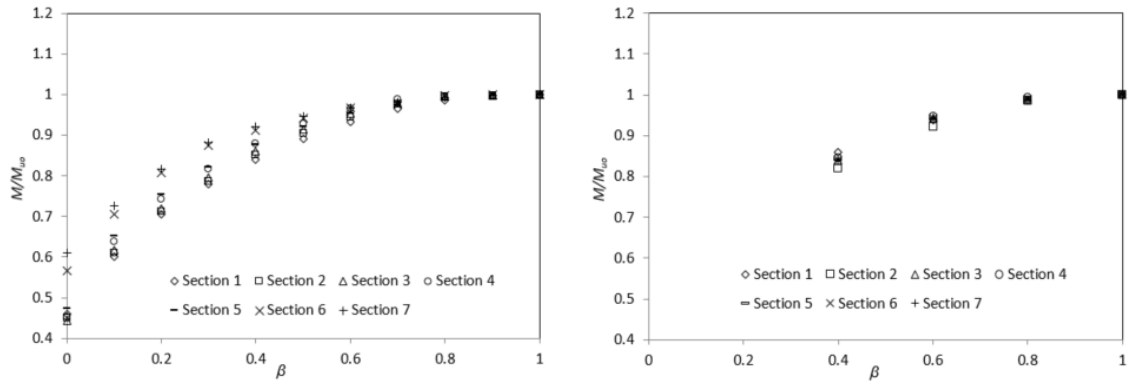

(a) RPA (b) CSA

Fig. 7 Effect of β on the pure sagging moment capacity

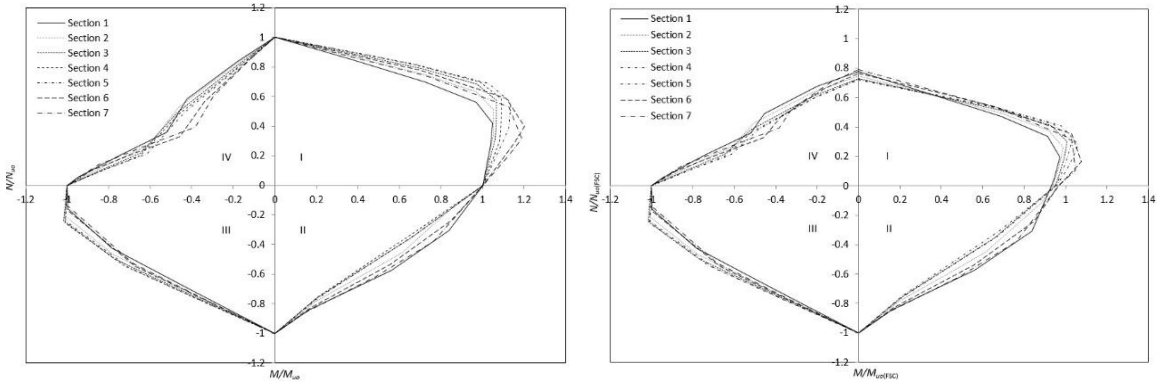

(a) Full shear connection β = 1.0 (b) Partial shear connection β = 0.6

Fig. 8 Rigid plastic analysis results of parametric beams

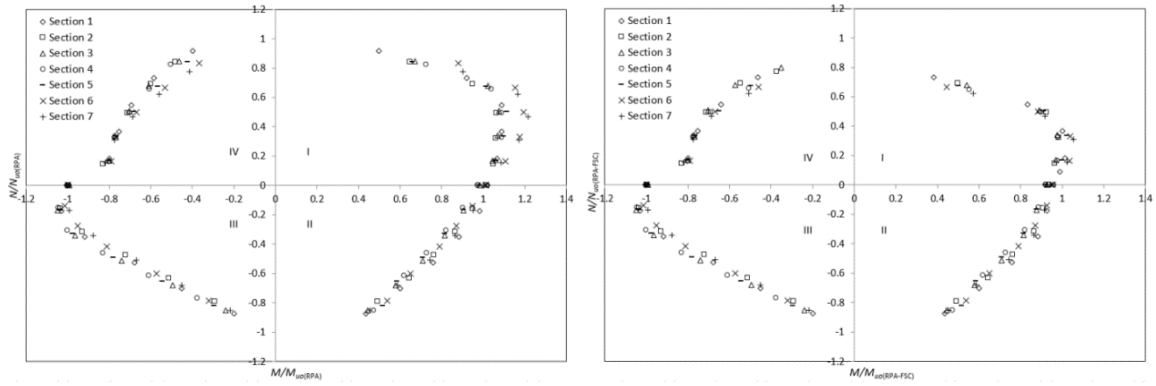

(a) Full shear connection β = 1.0 (b) Partial shear connection β = 0.6

Fig. 9 Cross-sectional analysis results of parametric beams

compressive flange when axial compression was added.

In Fig. 9(b), all values were non-dimensionalised using the values from the FSC case obtained in the RPA, $M_{uo(\text{RPA-FSC})}$ and $N_{uo(\text{RPA-FSC})}$. Similarly to the RPA results, the degree of shear connection did not affect the ultimate strength in quadrant III due to β having been designed for the positive bending case.

5. Design models

5.1 Axially loaded members

Vasdravellis *et al*. (2012a, b, c, 2014) previously proposed design models for estimating the moment-axial load interaction of composite beams. The design models are shown in Fig. 10 with comparison to the parametric beam results for FSC where M_{uo} and N_{uo} are determined by an RPA.

Vasdravellis *et al*. (2014) proposed design equations for use with beams subjected to sagging bending and compression where the axial compression load is distributed to the concrete slab. The CSA results presented in quadrant I of Fig. 10 show this model to be very conservative. However failure of the specimen in the CSA is only triggered due to exceeding the designated ultimate material strains at the mid-span, or when the designated ultimate slip value is exceeded at the ends of the specimen or at the hinge. The model does not consider a premature shear connection failure due to localised strains at the end of the beam. Nor does it consider a localised bearing failure. Both of these failure modes were noted during the experimental program when the axial load was applied directly to the steel section only. Buckling of the bottom flange was observed in specimen CB5 during experimental series 3. This specimen was subject to an axial compression load greater than the steel section's squash load capacity and suffered local buckling failure at the beam end. Specimens CB2 and CB3 of experimental series 4 suffered a premature shear connection failure. Nonetheless, the CSA results show that the design model may underestimate the flexural strength at mid- and high-compression loads and a change to the model above is proposed as

$$M \leq M_{uo}, \quad \text{for} \quad N \leq 0.6\, N_{uo} \tag{12}$$

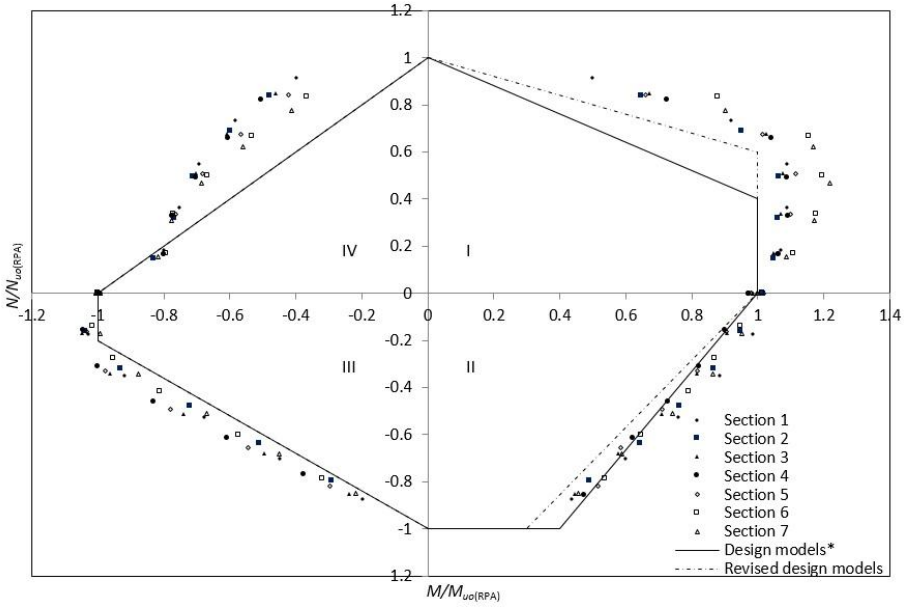

* Design models previously proposed by (Vasdravellis *et al*. 2012a, b, c, 2014)

Fig. 10 Design models and CSA results for FSC

$$\frac{N}{N_{uo}} + 0.4\frac{M}{M_{uo}} \leq 1, \qquad \text{for} \quad M > 0.6\,N_{uo} \tag{13}$$

The design model for sagging bending and tension in quadrant II was proposed by Vasdravellis *et al*. (2012b). This model is seen to slightly overestimate the flexural strength at large tensile loads. A change to the design model proposes an axial load unaffected for sagging moments less than 30% of M_{uo} to account for this overestimation of strength

$$N \leq N_{uo}\,, \qquad \text{for} \quad M \leq 0.3\,M_{uo} \tag{14}$$

$$0.7\frac{N}{N_{uo}} + \frac{M}{M_{uo}} \leq 1, \qquad \text{for} \quad M > 0.3\,M_{uo} \tag{15}$$

In quadrant III, the design model proposed by Vasdravellis *et al*. (2012a) is shown to be quite accurate. The model is

$$M \leq M_{uo}\,, \qquad \text{for} \quad N \leq 0.2\,N_{uo} \tag{16}$$

$$\frac{N}{N_{uo}} + 0.8\frac{M}{M_{uo}} \leq 1, \qquad \text{for} \quad M > 0.2\,N_{uo} \tag{17}$$

Lastly, the design model in quadrant IV was proposed by Vasdravellis *et al*. (2012c). The CSA model shows that the proposed design model may slightly overestimate the flexural strength at low compression loads. In this case, the CSA suffered a buckling failure. With additional buckling

restraints, the linear relationship proposed will be sufficiently accurate

$$\frac{N}{N_{uo}} + \frac{M}{M_{uo}} \leq 1 \tag{18}$$

5.2 Members with partial shear connection

The strength of a composite beam with partial interaction can be conveniently calculated by rigid plastic analysis. AS2327.1 (Standards Australia, 2003) provides equations for calculating the sagging moment capacity as a function of the degree of shear connection as shown previously. Continuous functions for $M_{\beta o}$ as determined by the RPA for the seven sections used in the parametric study can be seen in Fig. 11(a). AS2327.1 also provides conservative estimates of the sagging moment capacity at any degree of shear connection using linear and bilinear approximations. These are calculated by determining M_S, $M_{\beta.5}$ and M_{uo}, where M_s is the moment capacity of the steel section and $M_{\beta.5}$ is the moment capacity at β = 0.5. $M_{\beta o}$ is then approximated using linear interpolation for other connection strengths.

The CSA has showed previously that the RPA may overestimate the strength of a member with PSC by as much as 9%. Continuous functions for M_β may be estimated using the following proposed equation

$$\frac{M_{\beta o}}{M_{uo}} = 1 - \left(1 - \frac{M_s}{M_{uo}}\right)(1-\beta)^2 \tag{19}$$

Use of this equation provides an estimate of the sagging bending strength $M_{\beta o}$ at any degree of shear connection but requires calculating only M_s and M_{uo}. Continuous functions for $M_{\beta o}$ as determined by Eq. (19) for the seven sections used in the parametric study can be seen in Fig. 11(b). This equation shows a conservative estimate of the strength calculated using the AS2327.1 (Standards Australia 2003), especially at shear connection values less than 0.6. A comparison between the continuous functions, linear and bilinear approximations calculated using AS2327.1 as well as Eq. (19) is shown in Fig. 12(a)-(b). This equation provides a far more accurate estimation of the CSA results.

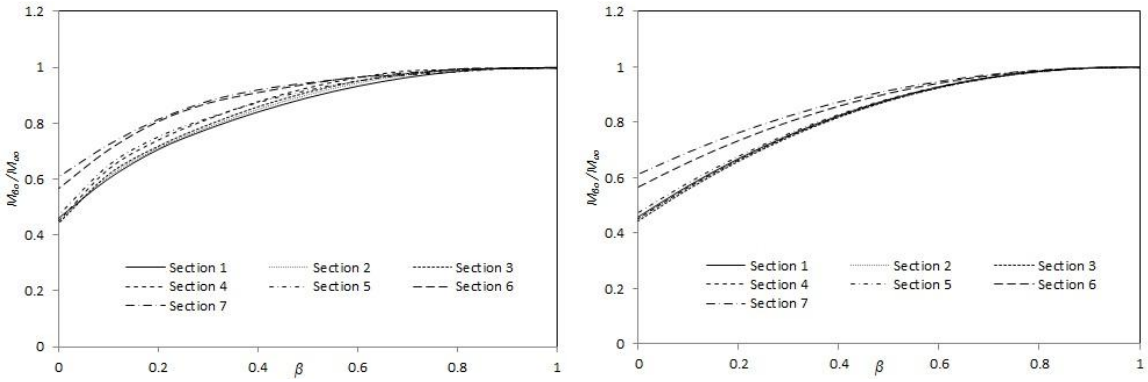

(a) Determined by AS2327.1 (b) Determined by Eq. (19)

Fig. 11 Continuous functions of $M_{\beta o}$

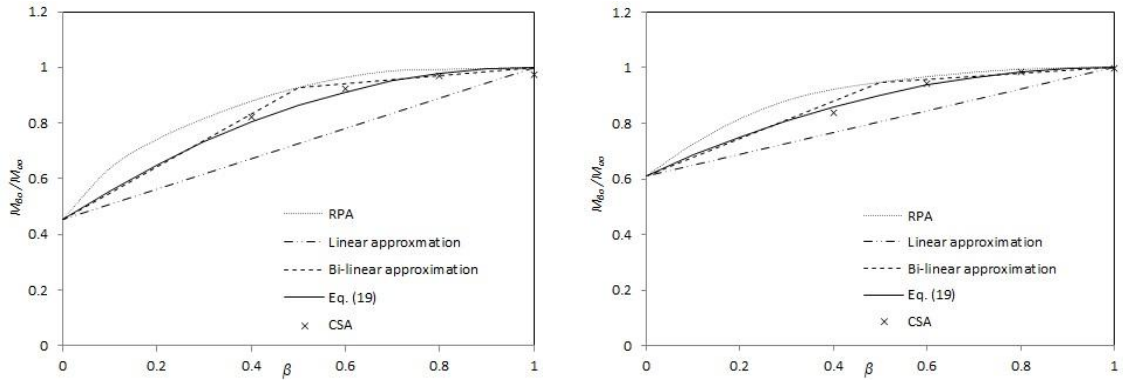

(a) Parametric section no. 4 (b) Parametric section no. 7

Fig. 12 $M_{\beta o}$ comparisons

5.3 Axially loaded members with partial shear connection

The proposed design models for axially loaded members may be adjusted to include the effect of PSC. This is achieved by reducing the pure moment capacity M_{uo} and pure axial capacity N_{uo} to $M_{\beta o}$ to $N_{\beta o}$ respectively. M_{uo} is reduced to $M_{\beta o}$ using the continuous functions provided by AS2327.1 (Standards Australia 2003) with Eq. (11) or by using the proposed Eq. (19). $N_{\beta o}$ is calculated by linearly reducing the squash load capacity N_{uo} with FSC to that of the bare steel section N_s at β = 0.0. The proposed model for sagging bending and compression shown in Eqs. (12)-(13), adjusted using the method for PSC, then becomes

$$M \leq M_{\beta o}, \quad \text{for} \quad N \leq 0.6\, N_{\beta o} \tag{20}$$

$$\frac{N}{N_{\beta o}} + 0.4\frac{M}{M_{\beta o}} \leq 1, \quad \text{for} \quad M > 0.6\, N_{\beta o} \tag{17}$$

Design models for *M–N* at various degrees of shear connection are shown in Fig. 13 using the equations referred to in the figure adjusted to include PSC. The pure moment capacity $M_{\beta o}$ in the figure is M_{uo} reduced by the average reduction in flexural strength determined by the RPA utilising Eq. (11). Likewise, the squash load $N_{\beta o}$ in the figure is N_{uo} reduced by the averages determined during the parametric study. Similar to the RPA and CSA results, the design models presented show no reduction in strength in quadrant III due to the degree of shear connection being designed for the sagging moment.

Fig. 14 presents comparisons between the CSA results and the design models for members with β = 0.6. The value of $M_{\beta o}$ used in the figure for the design models* is 0.956 which is the average reduction in the sagging moment capacity determined by the RPA for β = 0.6. It was shown previously that the use of Eq. (11) may overestimate the flexural strength. The average reduction in the pure moment capacity $M_{\beta o}$ for β = 0.6 and 0.4 determined by the RPA was 4.4% and 12% respectively. The CSA determined average reductions of 6% and 15.9% respectively. Use of Eq. (19) provides an average reduction of 8.1% and 18.2%. The revised design model in Fig. 14 uses $M_{\beta o}$ = 0.919 and a far better estimate of the strength can be seen in comparison to the CSA.

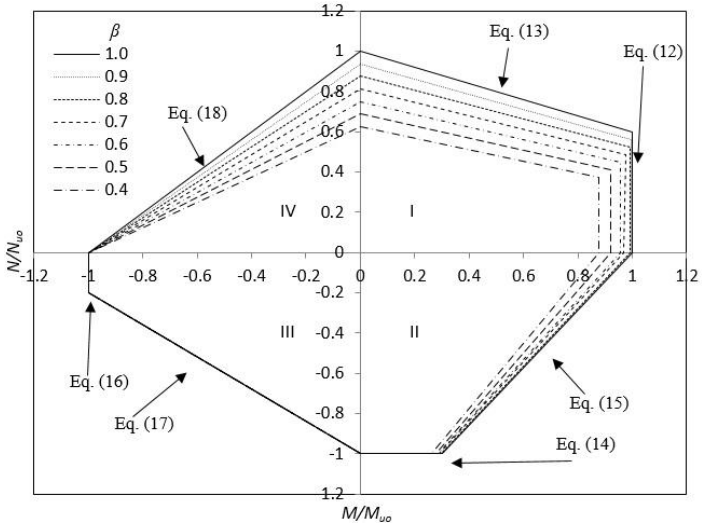

Fig. 13 Design models for moment-axial load interaction with PSC

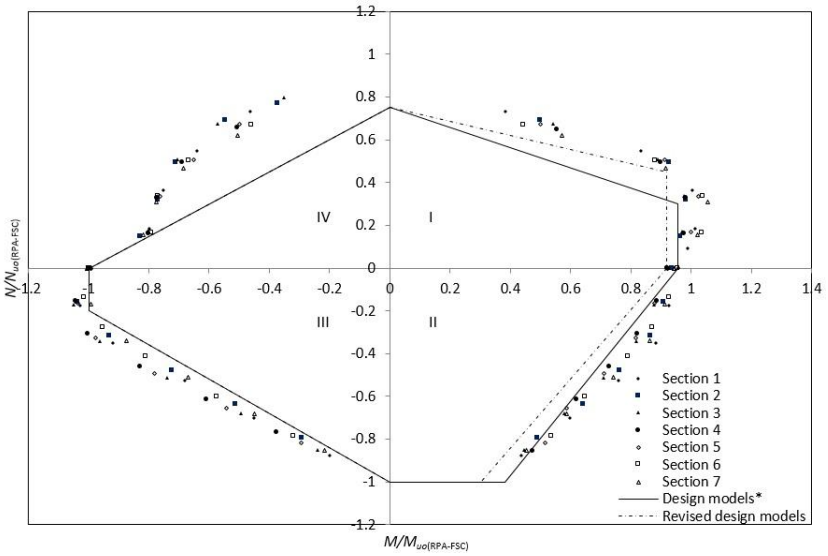

* Design models previously proposed by (Vasdravellis *et al*. 2012a, b, c, 2014)

Fig. 14 Design models and CSA results for β = 0.6

6. Conclusions

The analytical model developed herein was shown to provide accurate estimates of behaviour, strength and failure modes for composite beams subjected to flexure and axial load. Using the model, a set of parametric studies examining several key parameters was undertaken. The effect of axial load on the flexural strength of members and the effect of PSC on the sagging moment capacity of axially loaded members has been thoroughly explored.

The load-carrying capacity of a member is increased or decreased significantly depending on the direction and the location of the applied axial load as well as the deflection of the specimen. Extremely large deflections and vertical loads are achieved when high axial tension is introduced due to the ductile nature and large tensile strength of the steel beam. Specimen CB5 of series 1 reached a vertical load more than double that of the pure moment test of the same series. Likewise, specimen CB2 of series 2 reached a vertical point load 56% greater than that of specimen CB1. Conversely, compression loads are capable of dramatically reducing the load carrying capacity of a member. So much so that a flexural failure may occur without any additional vertical load, as shown by specimen CB4 of series 3.

The RPA has been shown to be a feasible design tool for axially loaded members with PSC. In most cases, the RPA produced results similar to but more conservative than the CSA and the experiments. However, some overestimation of strength occurred, particularly for the sagging bending and axial compression case with low degrees of shear connection. The flexural strength calculated by the AS2327.1 (Standards Australia 2003) continuous function was as much as 9% higher than that obtained by the CSA. The design equation proposed, Eq. (19), was shown to provide a far more accurate estimate of the strength in comparison with the CSA. Design models for estimating the *M–N* interaction of composite beams with full and partial interaction have been proposed. These design models show an excellent agreement with the CSA results and would be suitable for inclusion in future international design standards.

Acknowledgments

The authors wish to thank all the staff and students at University of Western Sydney's Institute for Infrastructure Engineering Structural Research and Testing Laboratory for their assistance in conducting the extensive experimental program. Funding provided by the Australian Research Council -Discovery Grant, DP087973 is also gratefully acknowledged.

References

Ayyub, B.M., Sohn, Y.G. and Saadatmanesh, H. (1992a), "Prestressed composite girders. I: Experimental study for negative moment", *J. Struct. Eng.*, **118**(10), 2743-2762.

Ayyub, B.M., Sohn, Y.G. and Saadatmanesh, H. (1992b), "Prestressed composite girders. II: Analytical study for negative moment", *J. Struct. Eng.*, **118**(10), 2763-2783.

British Standard Institution (2004), Eurocode 4, ENV 1994-1-1:1994, *Design of composite steel and concrete structures, Part 1.1 General rules and rules for buildings*, British Standard Institution, London, UK.

Carreira, D. and Chu, K. (1985), "Stress–strain relationship for plain concrete in compression", *J. Am. Concrete I.*, **82**(6), 797-804.

Chen, S. (2005), "Experimental study of prestressed steel-concrete composite beams with external tendons for negative moments", *J. Constr. Steel Res.*, **61**(12), 1613-1630.

Chen, S. and Gu, P. (2005), "Load carrying capacity of composite beams prestressed with external tendons under positive moment", *J. Constr. Steel Res.*, **61**(4), 515-530.

Chen, S., Wang, X. and Jia, Y. (2009), "A comparative study of continuous steel-concrete beams prestressed with external tendons: Experimental investigation", *J. Constr. Steel Res.*, **65**(7), 1480-1489.

Dundar, C., Tokgoz, S., Tanrikulu, A.K. and Baran, T. (2008), "Behaviour of reinforced and concrete-encased composite columns subjected to biaxial bending and axial load", *Build. Environ.*, **43**(6), 1109-

1120.
Elghazouli, A.Y. and Treadway, J. (2008), "Inelastic behaviour of composite members under combined bending and axial loading", *J. Constr. Steel Res.*, **64**(9), 1008-1019.
Huang, L., Lu, Y. and Shi, C. (2009), "Unified calculation method for symmetrically reinfored concrete section subjected to combined loading", *ACI Struct. J.*, **110**(1), 127-136.
Kaklauskas, G. and Ghaboussi, J. (2001), "Stress-strain relationship for cracked tensile concrete from RC beam tests", *J. Struct. Eng.*, **127**(1), 64-73.
Kemp, A.R. (1985), "Interaction of plastic local and lateral buckling", *J. Struct. Eng.*, **111**(10), 2181-2196.
Kemp, A.R. and Nethercot, D.A. (2001), "Required and available rotations in continuous composite beams with semi-rigid connections", *J. Constr. Steel Res.*, **57**(4), 375-400.
Liu, Y., Xu, L. and Grierson, D.E. (2009), "Combined MVP failure criterion for steel cross-sections", *J. Constr. Steel Res.*, **65**(1), 116-124.
Loh, H.Y., Uy, B. and Bradford, M.A. (2004a), "The effects of partial shear connection in the hogging moment regions of composite beams. Part I—Experimental study", *J. Constr. Steel Res.*, **60**(6), 897-919.
Loh, H.Y., Uy, B. and Bradford, M.A. (2004b), "The effects of partial shear connection in the hogging moment regions of composite beams. Part II—Analytical study", *J. Constr. Steel Res.*, **60**(6), 921-962.
Lorenc, W. and Kubica, E. (2006), "Behaviour of composite beams prestressed with external tendons: Experimental study", *J. Constr. Steel Res.*, **62**(12), 1353-1366.
Nguyen, Q.H., Hijaj, M., Uy, B. and Guezouli, S. (2009), "Analysis of composite beams in the hogging moment regions using a mixed finite element formulation", *J. Constr. Steel Res.*, **65**(3), 737-748.
Saadatmanesh, H., Albrecht, P. and Ayyub, B.M. (1989a), "Experimental study of prestressed composite beams", *J. Struct. Eng.*, **115**(9), 2348-2363.
Saadatmanesh, H., Albrecht, P. and Ayyub, B.M. (1989b), "Analytical study of prestressed composite beams", *J. Struct. Eng.*, **115**(9), 2364-2381.
Shanmugam, N.E. and Lakshmi, B. (2001), "State of the art steel-concrete composite columns", *J. Constr. Steel Res.*, **57**(10), 1041-1080.
Standards Australia (2003), *AS 2327.1-2003 Australian Standard*: *Composite Structures, Part 1*: *Simply Supported beams*, Standards Australia International Ltd.
Troitsky, M.S., Zielinski, Z.A. and Nouraeyan, A. (1989), "Pre-tensioned and post-tensioned composite girders", *J. Struct. Eng.*, **115**(12), 3142-3153.
Uy, B. and Bradford, M.A. (1993), "Cross-sectional deformation of prestressed composite tee-beams", *Struct. Eng. Rev.*, **5**(1), 63-70.
Uy, B. and Craine, S. (2004), "Static flexural behaviour of externally post-tensioned steel-concrete composite beams", *Adv. Struct. Eng.*, **7**(1), 1-20.
Uy, B. and Nethercot, D.A. (2005), "Effects of partial shear connection on the required and available rotations of semi-continuous composite beam systems", *Struct. Eng.*, **83**(4), 29-39.
Uy, B. and Tuem, H.S. (2006), "Behaviour and design of composite steel-concrete beams under combined actions", *ASCCS'2006 Eighth International Conference on Steel-Concrete Composite and Hybrid Structures*, Harbin, China, August.
Vasdravellis, G., Uy, B., Tan, E.L. and Kirkland, B. (2012a), "The effects of axial tension on the hogging-moment regions of composite beams", *J. Constr. Steel Res.*, **68**(1), 20-33.
Vasdravellis, G., Uy, B., Tan, E.L. and Kirkland, B. (2012b), "The effects of axial tension on the sagging-moment regions of composite beams", *J. Constr. Steel Res.*, **72**, 240-253.
Vasdravellis, G., Uy, B., Tan, E.L. and Kirkland, B. (2012c), "Behaviour and design of composite beams subjected to negative bending and compression", *J. Constr. Steel Res.*, **79**, 34-47.
Vasdravellis, G., Uy, B., Tan, E.L. and Kirkland, B. (2014), "Behaviour and design of composite beams subjected to sagging bending and compression", *J. Constr. Steel Res.*, **110**, 29-39.
Wu, Y.F., Oehlers, D.J. and Griffith, M.C. (2001a), "Numerical simulation of composite plated columns", Research Report No. R172, Dept. of Civil and Env. Engng, Adelaide University, Australia.
Wu, Y.F., Griffith, M.C. and Oehlers, D.J. (2001b), "Behaviour of plated RC columns", Research Report No. R173; Dept. of Civil and Env. Engng, Adelaide University, Australia.

Wu, Y.F., Oehlers, D.J. and Griffith, M.C. (2002), "Partial-interaction analysis of composite beam/column members", *Mech. Struct. Mach.*, **30**(3), 309-332.
Wu, Y.F., Griffith, M.C. and Oehlers, D.J. (2004), "Numerical simulation of steel plated RC columns", *Comp. Struct.*, **82**(4-5), 359-371.

CC